Published in final edited form as:
Neuroscience. 2010 June 16; 168(1): 288–299. doi:10.1016/j.neuroscience.2010.03.015.

Salicylate-induced degeneration of cochlea spiral ganglion neurons-apoptosis signaling

Lei Wei, **Dalian Ding**, and **Richard Salvi**
Center for Hearing and Deafness, University at Buffalo, Buffalo, NY 14214

Abstract

Aspirin, whose active ingredient is sodium salicylate, is the most widely used drugs worldwide, but it is not recommend for children because it may causes Reye's syndrome. High doses of salicylate also induce temporary hearing loss and tinnitus; while these disorders are believed to disappear when treatment is discontinued some data suggest that prolonged treatment may be neurotoxic. To investigate its ototoxicity, immature, postnatal day 3 rat cochlear organotypic cultures were treated with salicylate. Salicylate did not damage the sensory hair cells, but instead damaged the spiral ganglion neurons and their peripheral fibers in a dose-dependent manner. The cross sectional area of spiral ganglion neurons decreased from 205 μm^2 in controls to 143, 116 and 91 μm^2 in cultures treated with 1, 3 or 5 mM salicylate respectively. Morphological changes and caspase upregulation were indicative of caspase-mediated apoptosis. A quantitative RT-PCR apoptosis array identified a subset of genes up or down regulated by salicylate. Eight genes showed a biologically relevant change ($P < 0.05, \geq 2$ fold change) after 3 h treatment with salicylate; 7 genes (Tp53, Birc3, Tnfrsf5, Casp7, Nfkb1, Fas, Lta, Tnfsf10) were upregulated and 1 gene (Pycard) was downregulated. After 6 h treatment, only 1 gene (Nol3) was upregulated and 2 genes were downregulated (Cideb and Lhx4) while after 12 h treatment, 2 genes (Il10, Gadd45a) were upregulated and 4 (Prok2, Card10, Ltbr, Dapk1) were downregulated. High doses of salicylate in a physiologically relevant range can induce caspase-mediated cell death in immature spiral ganglion neurons; changes in the expression of apoptotic genes particularly among members of the TNF family appear to play an important role in the degeneration.

Keywords

aspirin; tumor necrosis factor; organotypic culture; PCR-array; caspase; NF-κB; postnatal

Introduction

Sodium salicylate (SS), the active component of aspirin, is one of the most widely used over the counter drugs for the treatment of pain, fever, inflammation, heart attacks, chest pain and a host of other health conditions (Lewis et al., 1983, Levine et al., 2005, Cheng, 2007). Aspirin has been implicated Reye's syndrome, a childhood disorder characterized by hyperammonemia and encephalopathy and which may involve mitochondrial permeability transition (Trost and Lemasters, 1996, Larsen, 1997). Long term consumption of high levels of SS can induce

Corresponding author: Richard Salvi, Center for Hearing and Deafness, University at Buffalo, 137 Cary Hall, Buffalo, NY 14214, Phone: 716 829 5310, Fax: 716 829 2980, salvi@buffalo.edu.

stomach bleeding, heart burn, nausea and vomiting (Levine et al., 1986). At high doses, SS can induce hearing loss and tinnitus, a phantom auditory sensation (Waltner, 1955, Vonweiss and Lever, 1964, Myers and Bernstein, 1965, Myers et al., 1965, Boettcher and Salvi, 1991). Although the ototoxic effects of salicylate have been well documented in humans and other mammals (Cazals, 2000, Yang et al., 2007), the biological mechanisms responsible for these disorders remain poorly understood. High doses of SS can impair neuronal function at multiple sites along the auditory pathway beginning with the outer hair cells (OHC) and spiral ganglion neurons (SGN) in the cochlea and progressing centrally to the auditory cortex (AC) (Chen and Jastreboff, 1995, Kakehata and Santos-Sacchi, 1996, Gao, 1999, Peng et al., 2003, Basta and Ernst, 2004, Wang et al., 2006, Basta et al., 2008). It is widely believed that the ototoxic effects of SS are temporary and completely reversible in adult animals (McFadden et al., 1984, Jung et al., 1993, Puel, 2007). This view is based largely on the fact that SS-induced hearing loss (audiometric threshold) and tinnitus seem to recover 24–48 h after cessation of treatment. However, recent in vivo studies from our lab suggest that chronic treatment with high levels of SS sufficient to induce tinnitus and hearing loss permanently reduces the neural output of the cochlea (Chen et al., Accepted). Previous in vitro studies indicate that SS can damage SGN neurites although the mechanisms underlying this neurotoxic effect are unknown (Zheng et al., 1997). Degeneration of SGN neurites occurs with salicylate concentrations similar to those found in the cerebral spinal fluid of rats with behavioral evidence of tinnitus (Jastreboff et al., 1986). Given aspirin's widespread use (Green, 2001, Heard et al., 2008) and its putative contribution to the encephalopathy associated with childhood Reye's syndrome (Larsen, 1997, Lemberg et al., 2009) there is substantial interest in determining whether the high doses of SS that induce tinnitus and hearing loss also lead to SGN degeneration. As a starting point for addressing this question, we applied SS to immature, postnatal cochlear organotypic cultures and evaluated the morphological changes and changes in apoptosis gene expression at 3, 6 and 12 h post-treatment.

Methods

Cochlear cultures

Cochlear organotypic cultures were prepared from postnatal day 3 SASCO Sprague Dawley rats as previously described (Ding et al., 2002, McFadden et al., 2003). Following decapitation, the cochlea was carefully removed and the organ of Corti and SGN were isolated and transferred onto rat tail collagen gel (type I rat-tail collagen (Collaborative Research, 3.76 mg/ml in 0.02 N acetic acid), 10×basal medium Eagle (BME) with 2% sodium carbonate in a 9:1:1 ratio). A 15-μL drop of the collagen gel was place onto the surface of a 35-mm culture dish and allowed to gel for approximately 30 min. Afterwards, 1.3 ml of culture medium (0.01 g/ml bovine serum albumin (BSA, Sigma A-4919), 1% Serum-Free Supplement (Sigma I-1884), 2.4% of 20% glucose (Sigma G-2020), 0.2% penicillin G (Sigma P-3414), 1% 200 mM glutamine (Sigma G-6392), 95.4% of 1× BME (Sigma B-1522)) was added to the dish. The cultures were subsequently transferred to an incubator (Forma Scientific 3029, 37 °C, 5% CO_2) for overnight incubation. On the following day, culture medium was replaced with new medium containing the desired compounds for the experimental treatments.

Salicylate Treatment

At the start of the salicylate treatment, normal culture medium was removed and replaced with medium containing 0.01 g/ml bovine serum albumin (BSA, Sigma A-4919), 1% Serum-Free Supplement (Sigma I-1884), 2.4% of 20% glucose (Sigma G-2020), 0.2% penicillin G (Sigma P-3414), 1% 200 mM glutamine (Sigma G-6392), 95.4% of 1× BME (Sigma B-1522) and various concentrations of salicylate (Sigma 71943, control, 1, 3, 5 or 10 mM). Afterwards, the cultures were placed in an incubator (Forma Scientific 3029, 37 °C, 5% CO_2) for a specified treatment period. At the end of the treatment, the cochlear cultures were removed from the dish

and fixed with 4% paraformaldehyde for 1 h and the tissue and collagen gel base were removed from the culture dish for staining and analysis.

Staining

Cochlear cultures were rinsed in 0.1 M PBS and immersed overnight at 4 °C in a solution containing a monoclonal antibody against neuronal class III β-tubulin (Covance, MMS-435P). The antibody was diluted 1:100 in blocking solution (Triton X-100 (1%), goat serum (3%), and 0.1 M PBS (96%)). The specimens were rinsed with 0.1 M PBS three times and incubated for 1 h with a secondary antibody labeled with Cy3 (goat anti-mouse IgG, Jackson ImmunoResearch Code: 115–165–206) dissolved in 0.1 M PBS (1:300). The specimens were rinsed with 0.1 M PBS and stained with Alexa 488-labeled phalloidin (Invitrogen A12379, diluted by 1:200) for 30 min. Specimens were rinsed with 0.1 M PBS and mounted on glass slides in glycerin and coverslipped.

A Polycaspase Assay Kit (Green, Neuromics, KF17200) was used to detect caspase activity (caspase-1, -3, -4, -5, -6, -7, -8 and -9). For SGN culture dish, 1 ml of serum-free culture medium with or without 5 mM SS was added to the treatment and control cultures, respectively. Cultures were incubated for 3 h followed by addition of 34 μl of 30X FAM-FLICA (1:30) working solution and incubation for 1 h. Specimens were then transferred to tubes with 0.9 ml freshly prepared 1X wash buffer and washed two times. Tissues were fixed for 30 min in 10% fixative (included in the kit). Specimens were then stained with a monoclonal antibody against neuronal class III β-tubulin as described above.

Confocal Microscopy

Specimens were examined with a confocal microscope (Zeiss LSM-510 meta, step size 0.5 μm per slice). For examination of SGN somas, 20–40 image planes were typically acquired; for hair cells and nerve fibers, 60–100 image planes were typically acquired. Unless specified, six samples or more were prepared for each experimental condition. Representative photomicrographs illustrating typical morphology were taken from the middle of each basilar membrane specimen. Images from multiple layers were projected onto a single plane using the Zeiss LSM Image Examiner (version: 4,0,0,91).

To quantify the shrinkage of SGN, the size of all SGN somata were calculated using the Zeiss LSM Image Examiner as follows. Multiple layers of the images were first merged onto a single layer. The number of layers merged was determined using two criteria: (1) the number of layers was maximized so that the largest cross sectional area of each SGN was included in analysis and (2) the overlap among different SGN was minimized. A polygon was drawn around the perimeter of the cell body of all distinguishable SGN and the Zeiss LSM Image Examiner (version: 4,0,0,91) automatically calculated the enclosed area. Data were evaluated for statistical significance with SigmaStat (version 3.5.0.54).

Cochleograms

Hair cell counts were obtained from cochlear cultures treated with 5 mM SS and from controls. Cochleograms were prepared as described previously (Ding, 2001). Briefly, specimens were fixed with 4% paraformaldehyde for 1 h, stained with Alexa 488-labeled phalloidin and examined under a fluorescence microscope (Zeiss Axioskop). The number of missing IHC and OHC were counted over 0.24 mm intervals along entire the length of the cochlea. Using lab norms (Ding et al., 2007), a cochleogram showing the percent hair cell loss as a function of percent distance from the apex was constructed for each sample. Results from controls and the 5 mM SS group were averaged (n=6/group) to obtain a mean cochleogram.

Quantitative RT-PCR

The SGN were carefully isolated from the organ of Corti and transferred into culture dishes containing culture medium (see above) with or without 5 mM SS. The numbers of cultures for each condition were 3 h control (10) SS (12); 6 h control (30) SS (32); 12 h control (44) SS (44). Cultures were placed in an incubator for 3, 6 or 12 h. Samples were harvested subsequently and total RNA (tRNA) was isolated and purified (RNeasy Lipid Tissue Mini Kit, QIAGEN 74804). Each sample of purified tRNA was diluted 1:100 in RNase-free water and examined on a spectrophotometer (Beckman Coulter DU640 Spectrophotometer; 260 nm/230 nm and 260 nm/280 nm) to test the purity and concentration (μg/ml) of RNA used for synthesis of first-strand complementary DNA (cDNA; RT^2 First Strand Kit, SABiosciences, C-03). The concentration of tRNA was used to ensure a consistent amount of tRNA (0.4 μg in this experiment) was used for cDNA production across all experimental conditions.

Expression of 84 apoptosis related genes were evaluated in control and SS-treated (5 mM, 3, 6 or 12 h duration) SGN samples in a 96-well plate (including 5 housekeeping and 7 control genes; Rat Apoptosis RT^2 Profiler™ PCR Array, SABiosciences, PARN-012A). Apoptosis gene arrays were processed according to the manufacturer's instructions. RT^{2}Real-Time™ SYBR Green/fluorescein PCR Master Mix (included in the kit) was used to monitor the fluorescence signal during each cycle of the PCR reaction. The apoptosis arrays were evaluated on a MyiQ™ Single-Color Real-Time PCR Detection System (BIO-RAD, Model No. MyiQ™ Optical Module). Each PCR reaction started with an initial denaturation cycle at 95 °C for 10 min, followed by 40 cycles consisting of 15 s at 95 °C for denaturating and 1 min at 60 °C for annealing. Each experimental condition was repeated three times. The threshold for calculating cycle threshold (Ct) values was calculated using MyiQ software (version: 1.0.410) automatically. When comparing multiple tests, a fixed threshold was assigned manually, as suggested by the manufacturer. The relative expression of each of the 84 apoptosis related genes was calculated using the $\Delta\Delta C_t$ method (Livak and Schmittgen, 2001). Ct values were transferred into Microsoft Excel (Microsoft Office 2003) and analyzed with Web-Based PCR Array Data Analysis (http://www.sabiosciences.com/pcr/arrayanalysis.php,SABiosciences) to determine the fold change and p value of each gene. Since all five housekeeping genes Rplp1, Hprt, Rpl13a, Ldha and Actb were very stable, with average fold change equal to or less than ±0.57 fold at all three time points (Table 1), the average of all five housekeeping genes was used as the reference to evaluate the change in apoptosis-related gene expression. Changes in gene expression are defined as positive or negative fold regulation values.

Results

SS Damages Nerve Fibers

Figure 1A–D illustrates the typical status of the hair cells and nerve fibers in control medium and cultures treated with 1, 3, or 5 mM of SS for 48 h or 10 mM SS for 96 h. Three rows of OHC and 1 row of IHC were present in the controls; many nerve fiber fascicles project radially and end near the IHC; a few fibers also project to the OHC (Figure 1A). Treatment with 1 mM SS had no noticeable effect on OHC or IHC; however, the density of nerve fiber fascicles projecting towards the hair cells was reduced. To quantify this effect, we measured the number of nerve fiber fascicles per 100 μm width in control and SS-treated samples. The numbers of nerve fiber fascicles were significantly (t-test, $p < 0.05$) reduced from 22.7 ± 1.0 (n=4) in controls to 14.6 ±0.8 (n=4) in the 1 mM SS treatment group. In addition, the distal ends of some fibers were slightly fragmented after 1 mM SS treatment (Figure 1B). After treatment with 5 mM SS, the number of nerve fiber fascicles decreased further to 12.5 ±0.3 (n=4) per 100 μm. Many beads and blebs were present on the surviving fibers (Figure 1C); however, the hair cells appeared normal (Figure 1C). Even after treatment for 96 h with 10 mM SS the hair cells appeared remarkably normal. However, many of the nerve fibers were missing and the

number of nerve fibers per 100 μm declined further to 3.9 ±1.3 (n=4) per 100 μm (Figure 1D). A one Way ANOVA showed that the overall treatment effect was significant (P = <0.001); multiple pair-wise comparisons using the Holm-Sidak method showed that all the pair were significant differences (P<0.05) except the comparison 1 mM vs. 5 mM SS.

Figure 1E–H shows the typical appearance of SGN cultured for 48 h in control medium or with 1, 3 or 5 mM of SS. The SGN in the control group had large, round or oval shaped cell bodies with thick neurites projecting from the soma (Figure 1E). Most SGN showed intense and uniform neurofilament labeling throughout the cytoplasm except for the nucleolus. After 48 h treatment with 1 mM SS, the soma of some SGN were shrunken; some showed only a slight decrease while others were nearly normal. Neurofilament labeling was relatively uniform throughout the cytoplasm and the neurites extending from the soma appeared normal (Figure 1F). After 48 h treatment with 3 mM SS, most SGN somas were dramatically reduced in size and most neurites were missing or extremely thin (Figure 1G). After 48 h treatment with 5 mM SS, the soma of nearly all SGN were greatly reduced in size and most SGN lacked neurites (Figure 1H). Neurofilament labeling of the cytoplasm tended to be less intense and less uniform compared to controls.

Cochleograms

Average cochleograms for the control group and group treated with 5 mM SS for 48 h were prepared to quantify the loss of hair cells (Figure 2). The mean loss of OHC and IHC was generally less than 5% along the basilar membrane for the control group (Figure 2A) and the group treated with 5 mM SS (Figure 2B). Since there was no obvious evidence of SS-induced hair cell loss for other conditions, even 10 mM SS after 96 h treatment, cochleograms were not prepared for other doses of SS.

SGN Size

Figure 4 shows the distribution of SGN soma cross sectional area in control samples and samples treated for 48 h with 1, 3 or 5 mM SS. In controls, the distribution is bimodal with two separate peaks; one peak (94% of sample) had a mode near 200 μm^2 and the second peak (6% of sample) had a mode near 80–90 μm^2. The two peaks are separated by a break near 100 μm^2. The distribution of SGN soma area gradually shifted towards smaller values with increase in SS dose (left side in Figure 3A). With 1 mM SS, the SGN major peak decreased to 160–170 μm^2 and the boundary between the small and large SGN became less distinct (Figure 3B). With 5 mM SS, more severe cell shrinkage occurred and the major peak was now located between 50 and 100 μm^2. However, a smaller peak was still present between 100 and 200 μm^2.

Figure 4 shows the mean SGN soma size (± SEM) of the control group and groups treated with 1, 3 or 5 mM SS for 48 h. SS treatment caused a dose dependent decrease in soma area. There was a statistically significant difference across the groups (P = <0.001, Kruskal-Wallis One Way Analysis) as well as a significant difference between the control and 1 mm SS groups (P <0.001), the 1 mM and 3 mM SS groups (P<0.001) and the 3 mM and 5 mM SS groups (P <0.001, Mann-Whitney Rank Sum Test).

SS Induces Caspase Activation

Soma shrinkage is a morphologic hallmark of apoptotic cell death (Wyllie et al., 1980, Bortner and Cidlowski, 1998, Maeno et al., 2000, Okada et al., 2001, Friis et al., 2005). Since caspases can play a critical role in apoptosis, cochlear cultures were treated for 3 h with 5 mM SS and labeled with a polycaspase fluorescent probe to determine if caspases were activated during the early stages of SS-induced cell death. SGN in control cultures had large, oval shaped somata, but were devoid of polycaspase activation (figure 5A). In contrast, the somas of many SGN treated with SS were shrunken and some of the shrunken SGN were polycaspase positive.

We counted the number of polycaspase positive and polycaspase negative somas in controls (n=5) and cultures treated for 3 h with 5 mm SS (n=5). Polycaspase labeling was absent from control cultures whereas 11.9 ±1.0% of SGN soma were polycaspase positive.

Apoptotic Gene Expression

To evaluate the mechanisms underlying SGN cell death, an apoptosis gene array containing 84 apoptosis related genes (Appendix 1) was used to identify significant changes in genes expression in SGN cultures treated with 5 mM SS for 3, 6 or 12 h. Table 1 lists the fold change in expression of the 84 apoptosis related genes at the three time points. The gray background was used to indicate genes that showed a biologically relevant change, operationally defined as an absolute fold change in expression equal to or greater than 2 (i.e., +2 or −2) as well as a statistically significant change in expression level ($P \leq 0.05$) relative to untreated controls.

At 3 h post-SS, eight genes were upregulated and only one gene was downregulated (Pycard). The three genes with the largest increase were Tnfsf10 (Fold change = 3.61, $P<0.05$), Lta (fold change = 2.80, $P<0.05$), and Fas (fold change = 2.65, $P<0.05$); all 3 belong to the tumor necrosis factor (TNF) family or their corresponding receptor genes. Tnfsf10 and Lta are both TNF-ligand genes, and Fas is a TNF-receptor gene; all three could be considered as pro-apoptotic. Nfkb1, which was upregulated 2.40 fold, plays important roles in apoptosis and cell proliferation. TNFRSF5, member 5 of the TNF receptor superfamily, was upregulated 2.16 fold; TNFRSF5 encodes for protein CD40, a receptor protein that acts as a key regulator in many immune responses (van Kooten and Banchereau, 2000, Xu and Song, 2004). Birc3 (baculoviral IAP repeat containing 3), which was upregulated 2.09 fold, belongs to the inhibitor of apoptosis (IAP) gene family capable of suppressing apoptosis by inhibiting caspases. Caspase 7, which was upregulated 2.36 fold, is an executor caspase that can be activated by initiator caspase 8. P53, a tumor suppressor gene, was also upregulated significantly (2.00 fold). The only gene that showed a biologically relevant down regulation was PYCARD (−2.22 fold). PYCARD encodes an adapter protein involved in the activation of caspases (Masumoto et al., 1999, Wang et al., 2002).

At 6 h post-SS, very few biologically relevant changes in apoptotic genes occurred. Only one gene, Nol3, was upregulated (2.08 fold). Nol3 encodes for nucleolar protein 3, which can inhibit caspase 8 (Koseki et al., 1998, Stoss et al., 1999). Cideb, a pro-apoptotic gene (Lugovskoy et al., 1999, Chen et al., 2000), was downregulated −2.05 fold. In addition, LHX4, which encodes the LIM/homeobox protein that functions as a transcriptional regulator (Machinis et al., 2001, Liu et al., 2002), was downregulated −2.03 fold.

At 12 h post-SS, four genes showed a significant downregulation. Prok2, which was downregulated −3.46, encodes the prokineticin 2 protein, which plays an important role in olfactory bulb neurogenesis and regulating circadian rhythms (Cheng et al., 2002, Ng et al., 2005). Card10, which was down regulated −3.38 fold, plays important roles in apoptosis through highly specific protein-protein homophilic interactions (McAllister-Lucas et al., 2001). Ltbr, which was down regulated −2.03 fold, encodes for lymphotoxin beta receptor protein, a member of tumor necrosis factor receptor family that triggers apoptosis. Dapk1, which was down regulated −2.01 fold, encodes for Death-associated protein kinase 1, a positive mediator of gamma-interferon induced programmed cell death (Feinstein et al., 1995, Hoek et al., 2008). Two genes were upregulated at 12 h post-SS. Interleukin-10, which was upregulated 2.15 fold, is an anti-inflammatory cytokine reported to block the activity of NF-κB (Park-Min et al., 2009). GADD45A, which was upregulated 2.22 fold, encodes for protein GADD45 alpha that is increased following DNA-damage (Hollander et al., 1993).

Discussion

The 1 and 3 mM doses of SS used this study are comparable to those observed in cochlear perilymph and cerebrospinal fluid of animals with hearing loss and tinnitus induced by systemic administration of a high dose of salicylate (Jastreboff et al., 1986, Jastreboff et al., 1988, Boettcher and Salvi, 1991, Lobarinas et al., 2006, Yang et al., 2007, Sun et al., 2009). Our results indicate that SS causes a dose-dependent shrinkage of SGN soma, a morphological feature of cells undergoing apoptosis, and a statistically significant loss of peripheral nerve fibers (Figure 1, 3, 4); these results are consistent with previous in vitro observations (Gao, 1999). Significant SGN soma shrinkage and significant loss of nerve fibers were seen with as little as 1 mM; this concentration is one-third of the dose previously shown to cause degeneration of SGN neurites (Gao, 1999). Given that the 1 mM dose caused a significant reduction (30%) in SGN soma size, it is conceivable that SGN toxicity could occur at sub-millimolar levels. In contrast to the neurotoxic effects, doses of SS ten fold higher (10 mM) failed to damage the hair cells, consistent with previous in vitro and in vivo studies (Gao, 1999, Yu et al., 2008, Yang et al., 2009). These results indicate that high doses of SS selectively damage the SGN, but do not damage the sensory hair cells. The lack of SS-induced outer hair cell damage in our cultures could conceivably be related to the low expression of prestin in postnatal outer hair cells (Gross et al., 2005, Abe et al., 2007); however this seems unlikely because long term SS treatment in vivo also does not lead to outer hair damage or impaired outer hair cell function (Huang et al., 2005, Chen et al., Accepted). The mechanisms underlying salicylate-induced SGN toxicity in our postnatal day 3 organotypic culture are not well understood. Since the cell bodies of the medial and lateral olivocochlear cochlear efferent neurons are severed during culture preparation, efferent neural activity is unlikely to be involved in SS-induced soma shrinkage. SS, however, is known to potentiate NMDA receptor currents in SGN raising the possibility that it leads to excitotoxicity (Guitton et al., 2003, Ruel et al., 2008).

Soma shrinkage

SS caused severe shrinkage of SGN soma (Figure 1, 3, 4), a morphological hallmark of apoptosis, and resulted in polycaspase activation (Wyllie et al., 1980,Maeno et al., 2000,Friis et al., 2005). Reductions in cell volume occur after activating TNFR1 with TNFα (Maeno et al., 2000). The TNFα-induced decrease in cell volume was prevented by blocking volume-regulated potassium or chloride currents which in turn inhibited apoptosis (Maeno et al., 2000). These results suggest SS-induced SGN soma shrinkage and nerve fiber loss might be prevented by blocking volume-regulatory chloride or potassium channels.

Gene signaling 3 h post-SS

SS induced biologically relevant changes in pro- and anti-apoptotic genes in SGN; these changes were used to develop a model (Figure 6) of SS-induced degenerative events in SGN. Eight genes showed a biologically relevant upregulation 3 h post-SS; 4 of these were members of the TNF family, namely Tnfsf10 (+3.61 fold, alias TRAIL), Lta (+2.80 fold), Fas (+2.65 fold) and Tnfrsf5 (+2.16 fold). The upregulation of these 4 genes are especially relevant because SS has been shown to enhance TNFα induced apoptosis in human pancreatic cancer cells (McDade et al., 1999).

Lta (alias: TNFSF1) encodes for Lymphotoxin alpha protein, a product of activated lymphocytes involved in many immune responses (Aggarwal et al., 1985, Aggarwal et al., 1987). Upregulation of Lta ligand was associated with a slight, but non-significant increase in its receptor, Ltbr (Lymphotoxin beta receptor) (1.34 fold, $P > 0.05$, Table 1) (Crowe et al., 1994). Tnfrsf5 (alias: CD40) is an integral receptor membrane protein expressed on a variety of cells. Upregulation of the Tnfrsf5 receptor was associated with a slight downregulation

(−1.21 fold, P > 0.05, Table 1) of its ligand, Tnfsf5 (alias: CD40LG). Since upregulation of Lta and Tnfrsf5 were not associated with a corresponding increase in their partners, it is unclear how they contribute to SS-induced SGN soma shrinkage and nerve fiber loss; therefore Lta and Tnfrsf5 were not incorporated in our model.

Upregulation of the Tnfsf10 ligand was accompanied by a large increase (1.97 fold, P < 0.05) in its receptor Tnfrsf10b (alias: TRAIL-R2). Likewise, the increase in the Fas receptor was associated with a moderate (1.58 fold, P < 0.05) increase in its ligand, Faslg. Since Fas and TRAIL (Tnfsf10) were upregulated in parallel with their partners, these 2 genes and their cohorts were incorporated into our model of SS-induced degenerative events in SGN (Figure 6).

The Fas ligand (Fas-L) encodes for a type II transmembrane protein (Oshimi et al., 1996, Nagata, 1999). When Fas-L binds to the Fas receptor, it causes oligomerization of Fas and forms a death-inducing signaling complex (DISC) (Itoh et al., 1991, Nagata, 1999). DISC transmits the apoptotic signal to its downstream pathway by recruiting Fas-associated protein with the death domain (FADD) (Figure 6), an adaptor molecule, to DISC (Cohen, 1997, MacFarlane, 2003). FADD was slightly upregulated (+1.36 fold, P > 0.05, Table 1) 3 h post-SS. FADD then cleaves procaspase 8 to its active form (Figure 6) (Cohen, 1997). Caspase 8 was significantly upregulated (+1.37 fold, P < 0.05, Table 1) 3 h post-SS. Rat caspase 8-associated protein 2 (Casp8ap2) was also significantly upregulated (+1.68 fold, P < 0.05). FLASH, the counterpart of murine Casp8ap2, is a component of DISC and involved in Fas-induced apoptosis (Imai et al., 1999).

Activated caspase 8 can lead to either to downstream activation of caspase 3 (−1.19 fold, P < 0.05, Table 1) or caspase 7 (+2.36 fold, P < 0.05, Table 1). The significant upregulation of caspase 7 (Figure 6) at 3 h post-SS presumably cleaves inhibitor of caspase-activated DNase (ICAD, alias: DFFA, DFF45, +1.21 fold, P > 0.05, Table 1) and releases caspase-activated DNase (CAD, alias: DFFB, DFF40, +1.45 fold, P>0.05, Table 1) which causes DNA degradation (Liu et al., 1997,Enari et al., 1998,Sakahira et al., 1998,Houde et al., 2004).

TNF-related apoptosis-inducing ligand (TRAIL) is a protein encoded by the TRAIL gene (+3.61 fold, P < 0.05, Table 1). Binding of TRAIL to apoptosis-inducing receptors TRAIL-R1 or TRAIL-R2 (alias: Tnfrsf10b, +1.97 fold, P<0.05) (Figure 6) triggers the trimerisation of the receptor and forms the death-inducing signaling complex (DISC) (Pan et al., 1997,Almasan and Ashkenazi, 2003). The adaptor protein FADD is recruited to DISC and convert pro-caspase 8 to active caspase 8. Thus, two distinct apoptotic pathways: one triggered by Fas-L and the other initiated by TRAIL, converge to activate FADD, which in turn activates caspase 8 (Figure 6).

BH3 interacting domain death agonist (Bid, +1.88 fold, P < 0.05, Table 1) is another substrate of caspase 8 (Haupt et al., 2003). Activated caspase 8 cuts Bid into tBid (Figure 6). After transport to the mitochondria, tBid induces Bax (+1.27 fold, P<0.05, Table 1) and Bak (+1.83 fold, P < 0.05, Table 1) to permeate the mitochondrial membrane resulting in the release of cytochrome c (Haupt et al., 2003).

TRAIL can also bind to TRAIL-R3 and TRAIL-R4; overexpression of TRAIL-R4 may be responsible for increased expression of NF-κB (+2.40 fold, P < 0.05, Table 1, Figure 6) (Hsu et al., 1996,Malinin et al., 1997,Degli-Esposti, 1999,Devin et al., 2000) Aspirin is known to increase expression of NF-κB protein by suppressing its inhibitor IκB (Loveridge et al., 2008). NF-κB can translocate to the nucleus and activate anti-apoptotic or apoptotic genes (Kucharczak et al., 2003,Dutta et al., 2006,Loveridge et al., 2008). The anti-apoptotic gene IAP-1 (alias Birc3 - Baculoviral IAP repeat-containing 3, +2.09 fold, P < 0.05, Table 1) was significantly upregulated 3 h post-SS. On the other hand, NF-κB can promote apoptosis by

enhancing the expression of Fas, which was upregulated by SS (Table 1) (Kasibhatla et al., 1999,Dutta et al., 2006,Loveridge et al., 2008). In addition, overexpression of c-Rel, a subunit of NF-κB, enhances TRAIL-induced apoptosis (Ghosh et al., 1998,Perkins, 2000,Baldwin, 2001,Chen et al., 2003) (Figure 6).

The p53 protein encoded by the Tp53 gene plays a key role in monitoring the integrity of the genome and inducing apoptosis in cells with damaged DNA (Matlashewski et al., 1984, Isobe et al., 1986, Kern et al., 1991, Haupt et al., 2003). P53 was significantly upregulated 3 h post-SS (Tp53, +2.00 fold, $P < 0.05$, Table 1); activation of p53 could occur as a result of membrane damage initiated through Fas and TRAIL and subsequent downstream signaling through the caspase 7-CAD pathway that results in DNA damage (Figure 6). Induction of p53 has also been reported to activate NF-κB (Ryan et al., 2000) (Figure 6).

Gene signaling 6 h and 12 h post-SS

The 8 genes that displayed a biologically relevant upregulation 3 h post-SS fell below our biologically relevant threshold at 6 h post-SS possibly due to the upregulation of anti-apoptotic genes such as Birc3 (+2.09 fold, $P< 0.05$) at 3 h post-SS. Nol3 (alias: ARC, +2.08 fold, $P <0.05$, Table 1) showed a biologically relevant increase 6 h post-SS. Nol3, which encodes for nucleolar protein 3, selectively interacts with caspase 8, but not caspase 3 or 9. By suppressing the enzyme activity of caspase 8, Nol3 inhibits Fas-induced apoptosis mediated by FADD and TRADD (Koseki et al., 1998,Stoss et al., 1999). This may explain why caspase 8 was attenuated between 3 h (+1.37 fold) and 6 h (+1.05 fold) whereas caspase 3 was enhanced between 3 h (−1.19 fold) and 6 h (+1.54 fold). Activation of caspase 3 may contribute to the late stage of SS-induced degenerative events in SGN.

Biologically relevant changes in gene expression at 12 h were similar to those at 6 h post SS. Most pro-apoptotic genes showed no difference in expression levels between control and SS-treated group. CAD (alias: DFF40 or DFFB; −1.58 fold, $P<0.05$, Table 1) and ICAD (alias: DFF45 or DFFA; −1.76 fold, $P<0.05$, Table 1) were further downregulated suggesting that these anti-apoptotic pathways were being upregulated.

Clinical Implications

Aspirin, whose active component is salicylate, is one of the most widely used over-the-counter medications; however, its is not recommended for use in children since it has been implicated in Reye's syndrome, a childhood disorder characterized by encephalopathy and hyperammonemia (Trost and Lemasters, 1997, Lemberg et al., 2009). Millions of patients (e.g. rheumatoid arthritis) chronically self-administer high doses of the aspirin for pain relief, inflammation and other health problems. High doses of aspirin and SS have long been known to cause hearing loss and tinnitus. Aspirin and SS-induced hearing loss and tinnitus are considered to be completely reversible problems that disappear within a few days after discontinuing use (McCabe and Dey, 1965, Myers and Bernstein, 1965). In vivo data indicate that chronic, high doses of SS are not toxic to hair cells which explain why otoacoustic emissions, which arise from OHC, completely recovery after cessation of treatment (Chen et al., 2009, Yang et al., 2009, Chen et al., Accepted). However, our in vitro data indicate that doses of SS in the 1–3 mM range cause significant SGN soma shrinkage and nerve fiber loss. SS concentrations of 1–3 mM in cerebrospinal fluid and inner ear cause temporary hearing loss and tinnitus (Jastreboff et al., 1986, Boettcher et al., 1990). Since the current study was performed in vitro using neonatal rat cochlear cultures; it is unclear if long-term treatment with high doses of SS results in SGN degeneration in vivo with adult animals. Although much of the existing literature suggests that high doses of SS only cause temporary effects on hearing, recent in vivo studies from our lab indicate that chronic, high-dose SS treatment is associated with a significant and persistent reduction in the compound action potential, a physiological

response that originates from auditory nerve and a significant, permanent reduction in the amplitude of the auditory brainstem response (Chen et al., Accepted). Taken together, these results suggest that long term treatment with high doses of salicylate is likely to exert neurotoxic effects on adult SGN. Since SGN loss and auditory nerve damage have little effect on behavioral thresholds, SS-induced damage to these structures may go undetected in routine audiometric thresholds assessment, but could lead to reductions in ABR amplitude as well as more subtle changes auditory performance such as poor speech perception or impaired temporal resolution (Schuknecht, 1994, Starr et al., 1996).

Supplementary Material

Refer to Web version on PubMed Central for supplementary material.

Acknowledgments

Supported in part by part by grants from NIH (R01DC009091; R01DC009219) and Tinnitus Research Initiative.

Abbreviations

SS	sodium salicylate
SGN	spiral ganglion neurons
CAP	compound action potential
TNF	tumor necrosis factor
OHC	outer hair cell
IHC	inner hair cell
Ct	cycle threshold
PCR	polymerase chain reaction
RT-PCR	reverse transcriptase PCR
AC	auditory cortex
BME	basal medium Eagle

References

Abe T, Kakehata S, Kitani R, Maruya S, Navaratnam D, Santos-Sacchi J, Shinkawa H. Developmental expression of the outer hair cell motor prestin in the mouse. J Membr Biol 2007;215:49–56. [PubMed: 17415610]

Aggarwal BB, Aiyer RA, Pennica D, Gray PW, Goeddel DV. Human tumour necrosis factors: structure and receptor interactions. Ciba Found Symp 1987;131:39–51. [PubMed: 2836139]

Aggarwal BB, Eessalu TE, Hass PE. Characterization of receptors for human tumour necrosis factor and their regulation by gamma-interferon. Nature 1985;318:665–667. [PubMed: 3001529]

Almasan A, Ashkenazi A. Apo2L/TRAIL: apoptosis signaling, biology, and potential for cancer therapy. Cytokine Growth Factor Rev 2003;14:337–348. [PubMed: 12787570]

Baldwin AS Jr. Series introduction: the transcription factor NF-kappaB and human disease. J Clin Invest 2001;107:3–6. [PubMed: 11134170]

Basta D, Ernst A. Effects of salicylate on spontaneous activity in inferior colliculus brain slices. Neurosci Res 2004;50:237–243. [PubMed: 15380332]

Basta D, Goetze R, Ernst A. Effects of salicylate application on the spontaneous activity in brain slices of the mouse cochlear nucleus, medial geniculate body and primary auditory cortex. Hear Res. 2008

Boettcher FA, Bancroft BR, Salvi RJ. Concentration of salicylate in serum and perilymph of the chinchilla. Arch Otolaryngol Head Neck Surg 1990;116:681–684. [PubMed: 2340120]

Boettcher FA, Salvi RJ. Salicylate ototoxicity: review and synthesis. Am J Otolaryngol 1991;12:33–47. [PubMed: 2029065]

Bortner CD, Cidlowski JA. A necessary role for cell shrinkage in apoptosis. Biochem Pharmacol 1998;56:1549–1559. [PubMed: 9973175]

Cazals Y. Auditory sensori-neural alterations induced by salicylate. Prog Neurobiol 2000;62:583–631. [PubMed: 10880852]

Chen G-D, Habiby Kermany M, D'Elia A, Ralli M, Tanaka C, Bielefeld EC, Ding D, Henderson D, Salvi R. Too much of a good thing: Long-term treatment with salicylate strengthens outer hair cell function but impairs auditory neural activity. Hear Res. (Accepted).

Chen G-D, Li M, Tanaka C, Bielefeld E, Kermany MH, Salvi R, Henderson D. Effect of Chronic Salicylate Treatment on Age-Related Cochlear Degeneration. Abstr Assoc Res Otolarygol 2009;32:197.

Chen GD, Jastreboff PJ. Salicylate-induced abnormal activity in the inferior colliculus of rats. Hear Res 1995;82:158–178. [PubMed: 7775282]

Chen X, Kandasamy K, Srivastava RK. Differential roles of RelA (p65) and c-Rel subunits of nuclear factor kappa B in tumor necrosis factor-related apoptosis-inducing ligand signaling. Cancer Res 2003;63:1059–1066. [PubMed: 12615723]

Chen Z, Guo K, Toh SY, Zhou Z, Li P. Mitochondria localization and dimerization are required for CIDE-B to induce apoptosis. J Biol Chem 2000;275:22619–22622. [PubMed: 10837461]

Cheng MY, Bullock CM, Li C, Lee AG, Bermak JC, Belluzzi J, Weaver DR, Leslie FM, Zhou QY. Prokineticin 2 transmits the behavioural circadian rhythm of the suprachiasmatic nucleus. Nature 2002;417:405–410. [PubMed: 12024206]

Cheng TO. The history of aspirin. Tex Heart Inst J 2007;34:392–393. [PubMed: 17948100]

Cohen GM. Caspases: the executioners of apoptosis. Biochem J 1997;326 (Pt 1):1–16. [PubMed: 9337844]

Crowe PD, VanArsdale TL, Walter BN, Ware CF, Hession C, Ehrenfels B, Browning JL, Din WS, Goodwin RG, Smith CA. A lymphotoxin-beta-specific receptor. Science 1994;264:707–710. [PubMed: 8171323]

Degli-Esposti M. To die or not to die--the quest of the TRAIL receptors. J Leukoc Biol 1999;65:535–542. [PubMed: 10331480]

Devin A, Cook A, Lin Y, Rodriguez Y, Kelliher M, Liu Z. The distinct roles of TRAF2 and RIP in IKK activation by TNF-R1: TRAF2 recruits IKK to TNF-R1 while RIP mediates IKK activation. Immunity 2000;12:419–429. [PubMed: 10795740]

Ding D, Jiang H, Wang P, Salvi R. Cell death after co-administration of cisplatin and ethacrynic acid. Hear Res 2007;226:129–139. [PubMed: 16978814]

Ding, D.; McFadden, S.; Salvi, RJ. Cochlear hair cell densities and inner ear staining techniques. In: Willott, JE., editor. The Auditory Psychobiology of the Mouse. CRC Press; Boca Raton: 2001. p. 189-204.

Ding D, Stracher A, Salvi RJ. Leupeptin protects cochlear and vestibular hair cells from gentamicin ototoxicity. Hear Res 2002;164:115–126. [PubMed: 11950531]

Dutta J, Fan Y, Gupta N, Fan G, Gelinas C. Current insights into the regulation of programmed cell death by NF-kappaB. Oncogene 2006;25:6800–6816. [PubMed: 17072329]

Enari M, Sakahira H, Yokoyama H, Okawa K, Iwamatsu A, Nagata S. A caspase-activated DNase that degrades DNA during apoptosis, and its inhibitor ICAD. Nature 1998;391:43–50. [PubMed: 9422506]

Feinstein E, Druck T, Kastury K, Berissi H, Goodart SA, Overhauser J, Kimchi A, Huebner K. Assignment of DAP1 and DAPK--genes that positively mediate programmed cell death triggered by IFN-gamma--to chromosome regions 5p12.2 and 9q34.1, respectively. Genomics 1995;29:305–307. [PubMed: 8530096]

Friis MB, Friborg CR, Schneider L, Nielsen MB, Lambert IH, Christensen ST, Hoffmann EK. Cell shrinkage as a signal to apoptosis in NIH 3T3 fibroblasts. J Physiol 2005;567:427–443. [PubMed: 15975986]

Gao WQ. Role of neurotrophins and lectins in prevention of ototoxicity. Ann N Y Acad Sci 1999;884:312–327. [PubMed: 10842603]

Ghosh S, May MJ, Kopp EB. NF-kappa B and Rel proteins: evolutionarily conserved mediators of immune responses. Annu Rev Immunol 1998;16:225–260. [PubMed: 9597130]

Green GA. Understanding NSAIDs: from aspirin to COX-2. Clin Cornerstone 2001;3:50–60. [PubMed: 11464731]

Gross J, Machulik A, Amarjargal N, Fuchs J, Mazurek B. Expression of prestin mRNA in the organotypic culture of rat cochlea. Hear Res 2005;204:183–190. [PubMed: 15925203]

Guitton MJ, Caston J, Ruel J, Johnson RM, Pujol R, Puel JL. Salicylate induces tinnitus through activation of cochlear NMDA receptors. J Neurosci 2003;23:3944–3952. [PubMed: 12736364]

Haupt S, Berger M, Goldberg Z, Haupt Y. Apoptosis - the p53 network. J Cell Sci 2003;116:4077–4085. [PubMed: 12972501]

Heard KJ, Ries NL, Dart RC, Bogdan GM, Zallen RD, Daly F. Overuse of non-prescription analgesics by dental clinic patients. BMC Oral Health 2008;8:33. [PubMed: 19068122]

Hoek KS, Schlegel NC, Eichhoff OM, Widmer DS, Praetorius C, Einarsson SO, Valgeirsdottir S, Bergsteinsdottir K, Schepsky A, Dummer R, Steingrimsson E. Novel MITF targets identified using a two-step DNA microarray strategy. Pigment Cell Melanoma Res 2008;21:665–676. [PubMed: 19067971]

Hollander MC, Alamo I, Jackman J, Wang MG, McBride OW, Fornace AJ Jr. Analysis of the mammalian gadd45 gene and its response to DNA damage. J Biol Chem 1993;268:24385–24393. [PubMed: 8226988]

Houde C, Banks KG, Coulombe N, Rasper D, Grimm E, Roy S, Simpson EM, Nicholson DW. Caspase-7 expanded function and intrinsic expression level underlies strain-specific brain phenotype of caspase-3-null mice. J Neurosci 2004;24:9977–9984. [PubMed: 15525783]

Hsu H, Huang J, Shu HB, Baichwal V, Goeddel DV. TNF-dependent recruitment of the protein kinase RIP to the TNF receptor-1 signaling complex. Immunity 1996;4:387–396. [PubMed: 8612133]

Huang ZW, Luo Y, Wu Z, Tao Z, Jones RO, Zhao HB. Paradoxical enhancement of active cochlear mechanics in long-term administration of salicylate. J Neurophysiol 2005;93:2053–2061. [PubMed: 15590729]

Imai Y, Kimura T, Murakami A, Yajima N, Sakamaki K, Yonehara S. The CED-4-homologous protein FLASH is involved in Fas-mediated activation of caspase-8 during apoptosis. Nature 1999;398:777–785. [PubMed: 10235259]

Isobe M, Emanuel BS, Givol D, Oren M, Croce CM. Localization of gene for human p53 tumour antigen to band 17p13. Nature 1986;320:84–85. [PubMed: 3456488]

Itoh N, Yonehara S, Ishii A, Yonehara M, Mizushima S, Sameshima M, Hase A, Seto Y, Nagata S. The polypeptide encoded by the cDNA for human cell surface antigen Fas can mediate apoptosis. Cell 1991;66:233–243. [PubMed: 1713127]

Jastreboff PJ, Brennan JF, Coleman JK, Sasaki CT. Phantom auditory sensation in rats: an animal model for tinnitus. Behav Neurosci 1988;102:811–822. [PubMed: 3214530]

Jastreboff PJ, Hansen R, Sasaki PG, Sasaki CT. Differential uptake of salicylate in serum, cerebrospinal fluid, and perilymph. Arch Otolaryngol Head Neck Surg 1986;112:1050–1053. [PubMed: 3755974]

Jung TT, Rhee CK, Lee CS, Park YS, Choi DC. Ototoxicity of salicylate, nonsteroidal antiinflammatory drugs, and quinine. Otolaryngol Clin North Am 1993;26:791–810. [PubMed: 8233489]

Kakehata S, Santos-Sacchi J. Effects of salicylate and lanthanides on outer hair cell motility and associated gating charge. J Neurosci 1996;16:4881–4889. [PubMed: 8756420]

Kasibhatla S, Genestier L, Green DR. Regulation of fas-ligand expression during activation-induced cell death in T lymphocytes via nuclear factor kappaB. J Biol Chem 1999;274:987–992. [PubMed: 9873041]

Kern SE, Kinzler KW, Bruskin A, Jarosz D, Friedman P, Prives C, Vogelstein B. Identification of p53 as a sequence-specific DNA-binding protein. Science 1991;252:1708–1711. [PubMed: 2047879]

Koseki T, Inohara N, Chen S, Nunez G. ARC, an inhibitor of apoptosis expressed in skeletal muscle and heart that interacts selectively with caspases. Proc Natl Acad Sci U S A 1998;95:5156–5160. [PubMed: 9560245]

Kucharczak J, Simmons MJ, Fan Y, Gelinas C. To be, or not to be: NF-kappaB is the answer--role of Rel/NF-kappaB in the regulation of apoptosis. Oncogene 2003;22:8961–8982. [PubMed: 14663476]

Larsen SU. Reye's syndrome. Med Sci Law 1997;37:235–241. [PubMed: 9264230]

Lemberg A, Fernandez MA, Coll C, Rosello DO, Romay S, Perazzo JC, Filinger EJ. Reyes's syndrome, encephalopathy, hyperammonemia and acetyl salicylic acid ingestion in a city hospital of Buenos Aires, Argentina. Curr Drug Saf 2009;4:17–21. [PubMed: 19149521]

Levine M, Wong D, Brown DF, Nadel ES. Chest pain and arthritis. J Emerg Med 2005;29:91–95. [PubMed: 15961016]

Levine MS, Verstandig A, Laufer I. Serpiginous gastric erosions caused by aspirin and other nonsteroidal antiinflammatory drugs. AJR Am J Roentgenol 1986;146:31–34. [PubMed: 3484407]

Lewis HD Jr, Davis JW, Archibald DG, Steinke WE, Smitherman TC, Doherty JE 3rd, Schnaper HW, LeWinter MM, Linares E, Pouget JM, Sabharwal SC, Chesler E, DeMots H. Protective effects of aspirin against acute myocardial infarction and death in men with unstable angina. Results of a Veterans Administration Cooperative Study. N Engl J Med 1983;309:396–403. [PubMed: 6135989]

Liu X, Zou H, Slaughter C, Wang X. DFF, a heterodimeric protein that functions downstream of caspase-3 to trigger DNA fragmentation during apoptosis. Cell 1997;89:175–184. [PubMed: 9108473]

Liu Y, Fan M, Yu S, Zhou Y, Wang J, Yuan J, Qiang B. cDNA cloning, chromosomal localization and expression pattern analysis of human LIM-homeobox gene LHX4. Brain Res 2002;928:147–155. [PubMed: 11844481]

Livak KJ, Schmittgen TD. Analysis of relative gene expression data using real-time quantitative PCR and the 2(-Delta Delta C(T)) Method. Methods 2001;25:402–408. [PubMed: 11846609]

Lobarinas E, Yang G, Sun W, Ding D, Mirza N, Dalby-Brown W, Hilczmayer E, Fitzgerald S, Zhang L, Salvi R. Salicylate- and quinine-induced tinnitus and effects of memantine. Acta Otolaryngol 2006; (Suppl):13–19.

Loveridge CJ, MacDonald AD, Thoms HC, Dunlop MG, Stark LA. The proapoptotic effects of sulindac, sulindac sulfone and indomethacin are mediated by nucleolar translocation of the RelA(p65) subunit of NF-kappaB. Oncogene 2008;27:2648–2655. [PubMed: 18059344]

Lugovskoy AA, Zhou P, Chou JJ, McCarty JS, Li P, Wagner G. Solution structure of the CIDE-N domain of CIDE-B and a model for CIDE-N/CIDE-N interactions in the DNA fragmentation pathway of apoptosis. Cell 1999;99:747–755. [PubMed: 10619428]

MacFarlane M. TRAIL-induced signalling and apoptosis. Toxicol Lett 2003;139:89–97. [PubMed: 12628743]

Machinis K, Pantel J, Netchine I, Leger J, Camand OJ, Sobrier ML, Dastot-Le Moal F, Duquesnoy P, Abitbol M, Czernichow P, Amselem S. Syndromic short stature in patients with a germline mutation in the LIM homeobox LHX4. Am J Hum Genet 2001;69:961–968. [PubMed: 11567216]

Maeno E, Ishizaki Y, Kanaseki T, Hazama A, Okada Y. Normotonic cell shrinkage because of disordered volume regulation is an early prerequisite to apoptosis. Proc Natl Acad Sci U S A 2000;97:9487–9492. [PubMed: 10900263]

Malinin NL, Boldin MP, Kovalenko AV, Wallach D. MAP3K-related kinase involved in NF-kappaB induction by TNF, CD95 and IL-1. Nature 1997;385:540–544. [PubMed: 9020361]

Masumoto J, Taniguchi S, Ayukawa K, Sarvotham H, Kishino T, Niikawa N, Hidaka E, Katsuyama T, Higuchi T, Sagara J. ASC, a novel 22-kDa protein, aggregates during apoptosis of human promyelocytic leukemia HL-60 cells. J Biol Chem 1999;274:33835–33838. [PubMed: 10567338]

Matlashewski G, Lamb P, Pim D, Peacock J, Crawford L, Benchimol S. Isolation and characterization of a human p53 cDNA clone: expression of the human p53 gene. EMBO J 1984;3:3257–3262. [PubMed: 6396087]

McAllister-Lucas LM, Inohara N, Lucas PC, Ruland J, Benito A, Li Q, Chen S, Chen FF, Yamaoka S, Verma IM, Mak TW, Nunez G. Bimp1, a MAGUK family member linking protein kinase C activation to Bcl10-mediated NF-kappaB induction. J Biol Chem 2001;276:30589–30597. [PubMed: 11387339]

McCabe PA, Dey FL. The Effect of Aspirin Upon Auditory Sensitivity. Ann Otol Rhinol Laryngol 1965;74:312–325. [PubMed: 14325847]

McDade TP, Perugini RA, Vittimberga FJ Jr, Carrigan RC, Callery MP. Salicylates inhibit NF-kappaB activation and enhance TNF-alpha-induced apoptosis in human pancreatic cancer cells. J Surg Res 1999;83:56–61. [PubMed: 10210643]

McFadden D, Plattsmier HS, Pasanen EG. Temporary hearing loss induced by combinations of intense sounds and nonsteroidal anti-inflammatory drugs. Am J Otolaryngol 1984;5:235–241. [PubMed: 6486350]

McFadden SL, Ding D, Salvemini D, Salvi RJ. M40403, a superoxide dismutase mimetic, protects cochlear hair cells from gentamicin, but not cisplatin toxicity. Toxicol Appl Pharmacol 2003;186:46–54. [PubMed: 12583992]

Myers EN, Bernstein JM. Salicylate ototoxicity; a clinical and experimental study. Arch Otolaryngol 1965;82:483–493. [PubMed: 4954319]

Myers EN, Bernstein JM, Fostiropolous G. Salicylate Ototoxicity: A Clinical Study. N Engl J Med 1965;273:587–590. [PubMed: 14329630]

Nagata S. Fas ligand-induced apoptosis. Annu Rev Genet 1999;33:29–55. [PubMed: 10690403]

Ng KL, Li JD, Cheng MY, Leslie FM, Lee AG, Zhou QY. Dependence of olfactory bulb neurogenesis on prokineticin 2 signaling. Science 2005;308:1923–1927. [PubMed: 15976302]

Okada Y, Maeno E, Shimizu T, Dezaki K, Wang J, Morishima S. Receptor-mediated control of regulatory volume decrease (RVD) and apoptotic volume decrease (AVD). J Physiol 2001;532:3–16. [PubMed: 11283221]

Oshimi Y, Oda S, Honda Y, Nagata S, Miyazaki S. Involvement of Fas ligand and Fas-mediated pathway in the cytotoxicity of human natural killer cells. J Immunol 1996;157:2909–2915. [PubMed: 8816396]

Pan G, O'Rourke K, Chinnaiyan AM, Gentz R, Ebner R, Ni J, Dixit VM. The receptor for the cytotoxic ligand TRAIL. Science 1997;276:111–113. [PubMed: 9082980]

Park-Min KH, Ji JD, Antoniv T, Reid AC, Silver RB, Humphrey MB, Nakamura M, Ivashkiv LB. IL-10 suppresses calcium-mediated costimulation of receptor activator NF-kappa B signaling during human osteoclast differentiation by inhibiting TREM-2 expression. J Immunol 2009;183:2444–2455. [PubMed: 19625651]

Peng BG, Chen S, Lin X. Aspirin selectively augmented N-methyl-D-aspartate types of glutamate responses in cultured spiral ganglion neurons of mice. Neurosci Lett 2003;343:21–24. [PubMed: 12749988]

Perkins ND. The Rel/NF-kappa B family: friend and foe. Trends Biochem Sci 2000;25:434–440. [PubMed: 10973057]

Puel JL. Cochlear NMDA receptor blockade prevents salicylate-induced tinnitus. B-ENT 2007;3(Suppl 7):19–22. [PubMed: 18225604]

Ruel J, Chabbert C, Nouvian R, Bendris R, Eybalin M, Leger CL, Bourien J, Mersel M, Puel JL. Salicylate enables cochlear arachidonic-acid-sensitive NMDA receptor responses. J Neurosci 2008;28:7313–7323. [PubMed: 18632935]

Ryan KM, Ernst MK, Rice NR, Vousden KH. Role of NF-kappaB in p53-mediated programmed cell death. Nature 2000;404:892–897. [PubMed: 10786798]

Sakahira H, Enari M, Nagata S. Cleavage of CAD inhibitor in CAD activation and DNA degradation during apoptosis. Nature 1998;391:96–99. [PubMed: 9422513]

Schuknecht HF. Auditory and cytocochlear correlates of inner ear disorders. Otolaryngol Head Neck Surg 1994;110:530–538. [PubMed: 8208568]

Starr A, Picton TW, Sininger Y, Hood LJ, Berlin CI. Auditory neuropathy. Brain 1996;119:741–753. [PubMed: 8673487]

Stoss O, Schwaiger FW, Cooper TA, Stamm S. Alternative splicing determines the intracellular localization of the novel nuclear protein Nop30 and its interaction with the splicing factor SRp30c. J Biol Chem 1999;274:10951–10962. [PubMed: 10196175]

Sun W, Lu J, Stolzberg D, Gray L, Deng A, Lobarinas E, Salvi RJ. Salicylate increases the gain of the central auditory system. Neuroscience 2009;159:325–334. [PubMed: 19154777]

Trost LC, Lemasters JJ. The mitochondrial permeability transition: a new pathophysiological mechanism for Reye's syndrome and toxic liver injury. J Pharmacol Exp Ther 1996;278:1000–1005. [PubMed: 8819478]

Trost LC, Lemasters JJ. Role of the mitochondrial permeability transition in salicylate toxicity to cultured rat hepatocytes: implications for the pathogenesis of Reye's syndrome. Toxicol Appl Pharmacol 1997;147:431–441. [PubMed: 9439738]

van Kooten C, Banchereau J. CD40-CD40 ligand. J Leukoc Biol 2000;67:2–17. [PubMed: 10647992]

Vonweiss JF, Lever WF. Percutaneous Salicylic Acid Intoxication in Psoriasis. Arch Dermatol 1964;90:614–619. [PubMed: 14208171]

Waltner JG. The effect of salicylates on the inner ear. Ann Otol Rhinol Laryngol 1955;64:617–622. [PubMed: 14388583]

Wang HT, Luo B, Zhou KQ, Xu TL, Chen L. Sodium salicylate reduces inhibitory postsynaptic currents in neurons of rat auditory cortex. Hear Res 2006;215:77–83. [PubMed: 16632286]

Wang L, Manji GA, Grenier JM, Al-Garawi A, Merriam S, Lora JM, Geddes BJ, Briskin M, DiStefano PS, Bertin J. PYPAF7, a novel PYRIN-containing Apaf1-like protein that regulates activation of NF-kappa B and caspase-1-dependent cytokine processing. J Biol Chem 2002;277:29874–29880. [PubMed: 12019269]

Wyllie AH, Kerr JF, Currie AR. Cell death: the significance of apoptosis. Int Rev Cytol 1980;68:251–306. [PubMed: 7014501]

Xu Y, Song G. The role of CD40-CD154 interaction in cell immunoregulation. J Biomed Sci 2004;11:426–438. [PubMed: 15153777]

Yang G, Lobarinas E, Zhang L, Turner J, Stolzberg D, Salvi R, Sun W. Salicylate induced tinnitus: behavioral measures and neural activity in auditory cortex of awake rats. Hear Res 2007;226:244–253. [PubMed: 16904853]

Yang K, Huang ZW, Liu ZQ, Xiao BK, Peng JH. Long-term administration of salicylate enhances prestin expression in rat cochlea. Int J Audiol 2009;48:18–23. [PubMed: 19173110]

Yu N, Zhu ML, Johnson B, Liu YP, Jones RO, Zhao HB. Prestin up-regulation in chronic salicylate (aspirin) administration: an implication of functional dependence of prestin expression. Cell Mol Life Sci 2008;65:2407–2418. [PubMed: 18560754]

Zheng XY, Henderson D, Hu BH, McFadden SL. Recovery of structure and function of inner ear afferent synapses following kainic acid excitotoxicity. Hear Res 1997;105:65–76. [PubMed: 9083805]

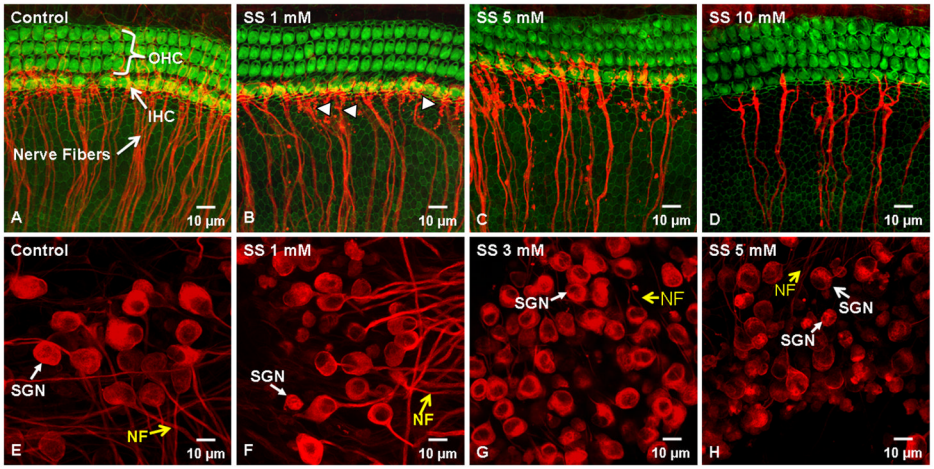

Figure 1.

Representative confocal photomicrographs of control and SS-treated cochlear organotypic cultures stained with Alexa 488-labeled phalloidin (green) to label hair cells and a monoclonal antibody against class III β-tubulin (red) to label SGN and their fibers projecting to the hair cells. (A) Control group with 3 rows of OHC and 1 row of IHC; note many nerve fiber fascicles projecting radially towards the IHC. (B) 1 mM (48 h) SS did not damage the hair cells. Density of radial nerve fibers decreased slightly; some fibers were fragmented (arrowheads). (C) Treatment with 5 mM (48 h) SS significantly reduced the number of nerve fiber fascicles; many blebs present on remaining fibers. (D) 10 mM SS (96 h) had no effect on hair cells, but greatly reduced the number of nerve fiber fascicles. (E) Control group with large, oval-shaped SGN soma and nerve fibers (yellow arrow). (F) After 1 mM SS, somas of many SGN were significantly smaller; neurites extending from soma were thinner than normal or absent. (G) 3 mM SS caused severe shrinkage of most of SGN; neurites missing from most SGN. (H) 5 mM SS (48 h) dramatically decreased SGN size; most neurites missing or extremely thin (yellow arrow).

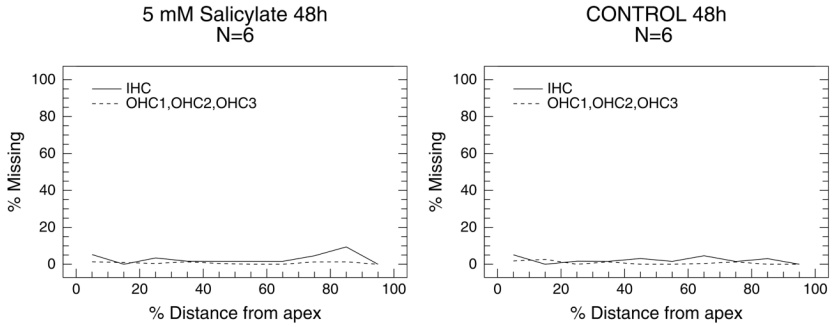

Figure 2.
Mean cochleogram showing percent IHC loss (solid line) and OHC loss (dashed line, OHC rows 1, 2, 3) in the control group (A) and group treated with 5 mM SS for 48 h (B).

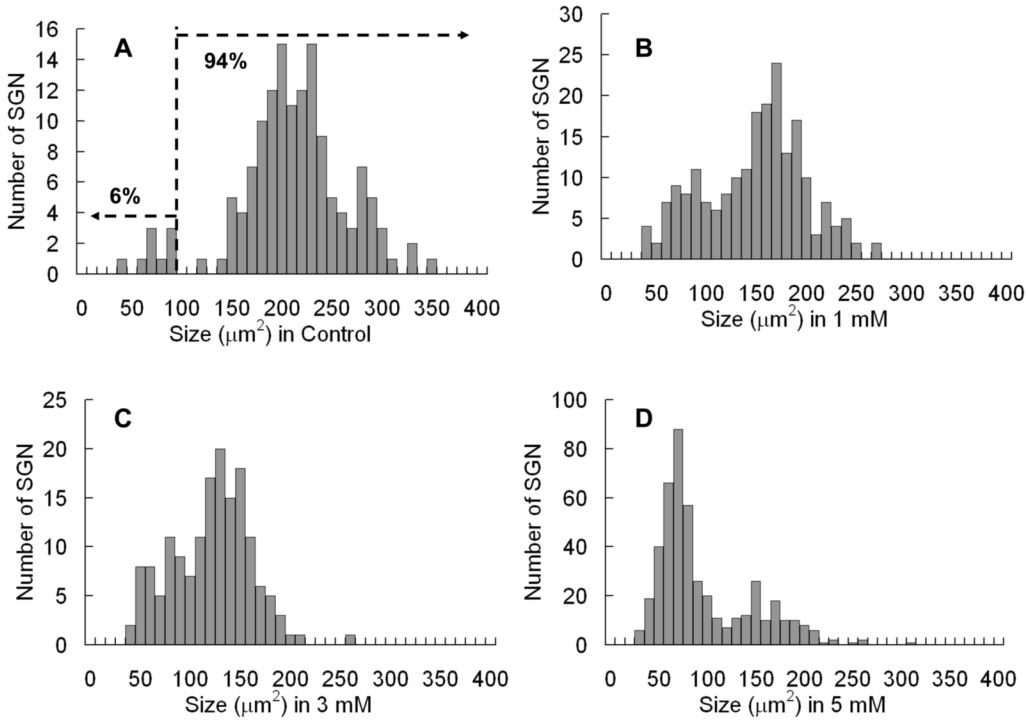

Figure 3.
Distributions of SGN soma size 48 h with various levels of SS treatment.

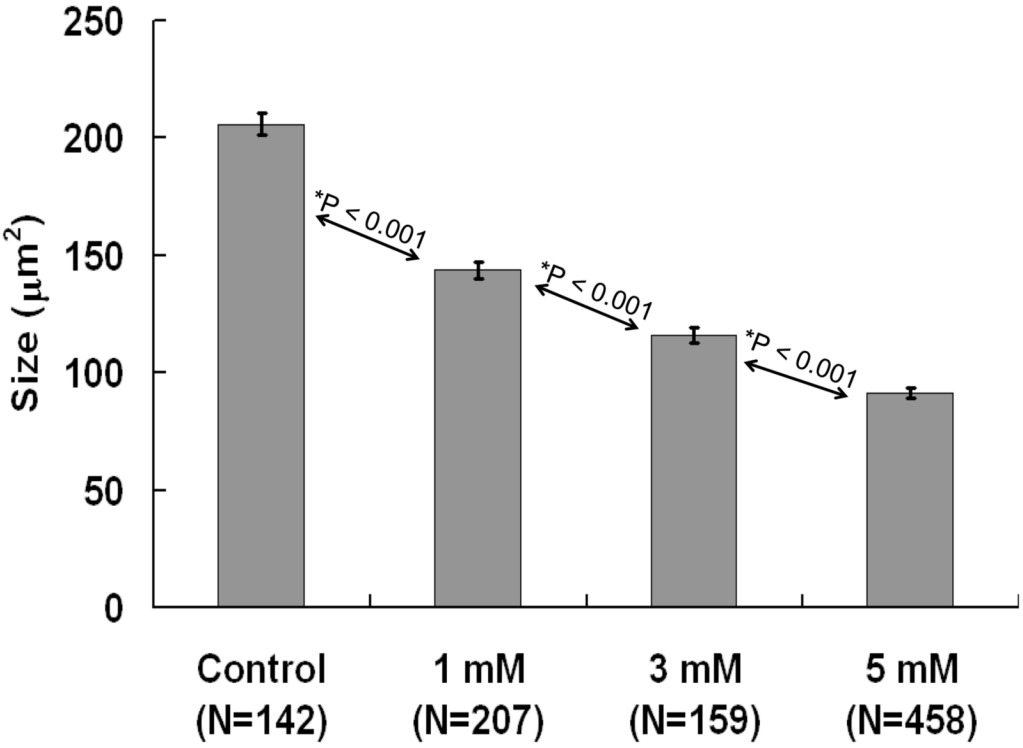

Figure 4.

Average soma size (±SEM) of SGNs in controls and cultures treated with 1, 3, and 5 mM SS for 48 h. Treatment effect statistically significant (Kruskal-Wallis One Way Analysis, P = <0.001); individual groups significantly different from one another (Mann-Whitney Rank Sum Test, p<0.001).

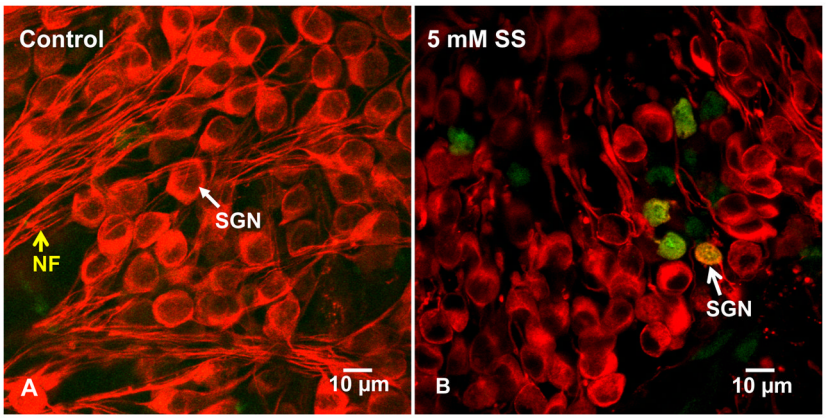

Figure 5.

Typical confocal photomicrographs of SGN stained with Polycaspase Assay Kit (green) and with antibody against neuronal III β-tubulin stain (red) to identify SGN. (A) In control cultures, most SGN have large, oval shaped soma and neurites extending from the soma; note absence of polycaspase labeling (green). (B) SGN treated for 3 h with 5 mM SS; polycaspase labeling was present on SGN with shrunken soma.

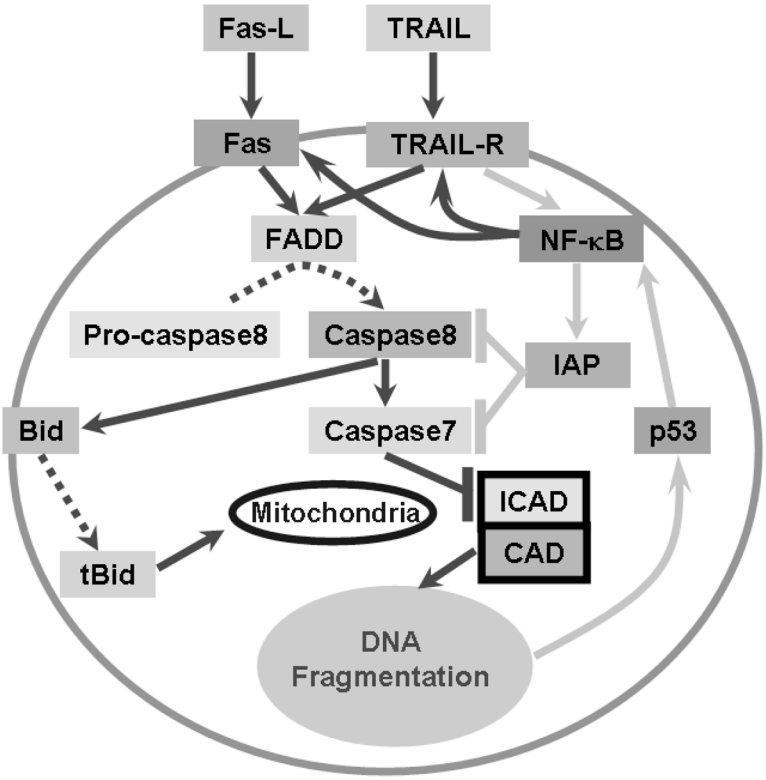

Figure 6.

Hypothesized SGN cell death pathways induced by 5 mM SS. Solid lines with arrowhead show gene activation; dotted lines with arrowhead indicate conversion of inactive to active processes; '⊦' indicates inhibition. Pro-apoptotic pathways were connected with dark lines and anti-apoptotic pathways are connected with light lines.

Table 1

Gene fold regulation with P value post-treatment of 5 mM SS (3 h: N= 10 C/12 SS; 6 h: N= 30 C/32 SS; 12 h: N = 44 C/44 SS)

Gene Symbol	Fold 3 h	P 3 h	Fold 6 h	P 6 h	Fold 12 h	P 12 h	Gene Symbol	Fold 3 h	P 3 h	Fold 6 h	P 6 h	Fold 12 h	P 12 h
Apaf1	−1.36	0.03	1.01	0.94	1.22	0.14	CAD	1.45	0.08	−1.54	0.21	−1.58	0.05
Api5	−1.19	0.01	−1.28	0.03	−1.15	0.07	Fadd	1.36	0.10	−1.02	0.85	−1.26	0.14
Aven	1.05	0.59	−1.35	0.05	−1.06	0.29	Faim	1.32	0.03	−1.10	0.68	1.28	0.04
Bad	1.03	0.70	1.01	0.89	−1.07	0.45	Gadd45a	−1.03	0.66	1.30	0.19	2.22	0.00
Bag1	1.09	0.41	1.06	0.60	1.02	0.82	Il10	1.44	0.02	1.17	0.04	2.15	0.04
Bak1	1.83	0.00	−1.24	0.02	−1.47	0.04	Lhx4	1.30	0.35	−2.03	0.02	−1.42	0.35
Bax	1.27	0.00	−1.12	0.10	−1.63	0.02	Lta	2.80	0.00	−2.23	0.10	−1.05	0.91
Bcl10	−1.08	0.32	1.06	0.67	−1.09	0.28	Ltbr	1.34	0.07	−1.01	0.85	−2.03	0.02
Bcl2	1.28	0.01	−1.24	0.22	−1.20	0.22	Mapk8ip	−1.05	0.50	−1.34	0.03	−1.67	0.01
Bcl2a1	−1.02	0.89	−1.15	0.06	1.24	0.16	Mcl1	−1.46	0.03	−1.21	0.06	−1.36	0.09
Bcl2l1	1.02	0.84	−1.48	0.00	−1.33	0.22	Nfkb1	2.40	0.00	−1.19	0.20	−1.70	0.03
Bcl2l11	−1.13	0.10	−1.09	0.80	−1.15	0.51	Nol3	−1.33	0.06	2.08	0.00	1.44	0.01
Bcl2l2	1.47	0.00	1.03	0.82	−1.72	0.08	Polb	1.19	0.10	−1.13	0.38	1.09	0.12
Bclaf1	−1.01	0.95	−1.41	0.01	−1.30	0.01	Prdx2	−1.28	0.02	−1.06	0.68	1.13	0.23
Bid	1.88	0.00	−1.08	0.37	−1.27	0.35	Prlr	−1.21	0.06	−1.07	0.33	1.26	0.10
Bid3	1.30	0.14	−1.03	0.83	1.01	0.93	Prok2	1.45	0.04	−1.86	0.01	−3.46	0.04
Bik	1.65	0.03	1.29	0.02	−1.08	0.51	Pycard	−2.22	0.00	−1.67	0.00	1.24	0.02
Birc1b	1.14	0.48	−1.22	0.27	1.06	0.58	Ripk2	1.52	0.01	1.25	0.14	1.18	0.11
Birc3	2.09	0.00	1.24	0.16	1.38	0.10	Sphk2	1.19	0.14	−1.12	0.28	1.06	0.59
Birc4	1.09	0.30	1.08	0.51	1.10	0.49	Tnf	−1.82	0.00	−1.46	0.01	−1.26	0.04
Birc5	−1.27	0.01	−1.06	0.47	−1.03	0.74	Tnfrsf10b	1.97	0.00	−1.11	0.35	−1.17	0.25
Bnip1	1.16	0.10	−1.07	0.38	1.02	0.77	Tnfrsf11b	1.19	0.05	−1.58	0.03	−1.35	0.13
Bnip2	−1.09	0.23	−1.19	0.03	−1.36	0.02	Tnfrsf1a	1.26	0.08	−1.08	0.45	−1.07	0.49
Bnip3	1.52	0.02	1.75	0.12	1.09	0.28	Tnfrsf1b	1.86	0.00	1.07	0.73	1.08	0.64
Bok	1.06	0.65	−1.17	0.05	−1.41	0.00	Tnfrsf5	2.16	0.00	1.13	0.51	1.44	0.08
Card10	−1.62	0.01	−1.75	0.02	−3.38	0.00	Fas	2.65	0.00	−1.08	0.62	1.21	0.35
Card6	1.39	0.02	1.05	0.72	−1.02	0.91	Tnfsf10	3.61	0.00	1.35	0.03	−1.19	0.45
Casp1	1.11	0.56	1.49	0.22	1.45	0.19	Tnfsf12	−1.33	0.03	−1.08	0.56	−1.13	0.41
Casp4	1.20	0.03	1.81	0.00	1.82	0.00	Cd40lg	−1.21	0.06	−1.07	0.33	1.26	0.10

Gene Symbol	Fold 3 h	P 3 h	Fold 6 h	P 6 h	Fold 12 h	P 12 h	Gene Symbol	Fold 3 h	P 3 h	Fold 6 h	P 6 h	Fold 12 h	P 12 h
Casp12	1.15	0.03	1.28	0.00	1.27	0.15	Faslg	1.58	0.02	−1.77	0.01	−1.18	0.33
Casp14	−1.21	0.06	−1.07	0.33	1.26	0.10	Tp53	2.00	0.01	−1.38	0.21	−1.40	0.02
Casp2	1.29	0.05	1.03	0.46	−1.25	0.31	Tradd	1.13	0.45	1.30	0.14	1.16	0.21
Casp3	−1.19	0.03	1.54	0.01	1.21	0.16	Traf1	1.72	0.02	1.81	0.02	1.08	0.75
Casp6	−1.29	0.00	−1.02	0.80	1.07	0.64	Traf2	1.66	0.00	1.09	0.19	−1.30	0.25
Casp7	2.36	0.00	1.06	0.80	−1.17	0.36	Traf3	1.33	0.05	−1.02	0.89	−1.50	0.06
Casp8	1.37	0.03	1.05	0.67	−1.17	0.09	Traf4	1.17	0.04	1.17	0.18	−1.21	0.21
Casp8ap2	1.68	0.04	1.24	0.62	1.06	0.64	Trp53bp2	−1.02	0.75	−1.22	0.24	−1.21	0.23
Casp9	1.22	0.13	−1.17	0.45	−1.34	0.15	Trp63	−1.09	0.46	−1.20	0.09	1.24	0.15
Cflar	1.31	0.18	−1.01	0.83	1.14	0.11	Trp73	−1.21	0.06	−1.08	0.31	1.26	0.10
Cidea	−1.10	0.43	−1.17	0.30	−1.15	0.27	Rplp1	−1.37	0.00	1.17	0.08	1.30	0.10
Cideb	1.24	0.44	−2.05	0.03	−2.08	0.10	Hprt	1.15	0.07	1.08	0.29	1.13	0.33
Cradd	−1.07	0.24	1.42	0.05	1.38	0.01	Rpl13a	−1.20	0.01	1.07	0.53	1.20	0.02
Dad1	−1.01	0.86	1.35	0.03	1.46	0.01	Ldha	1.57	0.00	1.10	0.15	−1.52	0.01
Dapk1	1.64	0.03	−1.15	0.47	−2.01	0.05	Actb	−1.10	0.19	−1.48	0.00	−1.16	0.08
ICAD	1.21	0.09	−1.41	0.05	−1.76	0.04							